Acetylation-dependent regulation of BRAF oncogenic function

Xiangpeng Dai[1,2,3,*], **Xiaoling Zhang**[2,3], **Qing Yin**[4], **Jia Hu**[1,5], **Jianping Guo**[1,6], **Yang Gao**[1,7], **Aidan H. Snell**[4], **Hiroyuki Inuzuka**[1], **Lixin Wan**[4,*], **Wenyi Wei**[1,8,*]

[1]Department of Pathology, Beth Israel Deaconess Medical Center, Harvard Medical School, Boston, MA 02215, USA

[2]Laboratory of Organ Regeneration & Transplantation of the Ministry of Education, The First Hospital of Jilin University, Changchun 130061, PR China

[3]National-local Joint Engineering Laboratory of Animal Models for Human Diseases, Changchun, Jilin 130061, PR China

[4]Department of Molecular Oncology, H. Lee Moffitt Cancer Center and Research Institute, 12902 USF Magnolia Drive, Tampa, FL 33612, USA

[5]Department of Urology, Tongji Hospital, Tongji Medical College, Huazhong University of Science and Technology, Liberalization Avenue, No. 1095, Wuhan 430030, PR China

[6]The First Affiliated Hospital, Sun Yat-sen University, Guangzhou 510275, PR China

[7]Department of Urology, The First Affiliated Hospital of Xi'an Jiaotong University, Xi'an 710061, PR China

[8]Lead contact

SUMMARY

Aberrant BRAF activation, including the BRAF^{V600E} mutation, is frequently observed in human cancers. However, it remains largely elusive whether other types of post-translational modification(s) in addition to phosphorylation and ubiquitination-dependent regulation also modulate BRAF kinase activity. Here, we report that the acetyltransferase p300 activates the BRAF kinase by promoting BRAF K601 acetylation, a process that is antagonized by the deacetylase SIRT1. Notably, K601 acetylation facilitates BRAF dimerization with RAF proteins and KSR1. Furthermore, K601 acetylation promotes melanoma cell proliferation and contributes to BRAF^{V600E} inhibitor resistance in *BRAF*^{V600E} harboring melanoma cells. As such, melanoma patient-derived K601E oncogenic mutation mimics K601 acetylation to augment BRAF

*Correspondence: daixiangpeng@jlu.edu.cn (X.D.), lixin.wan@moffitt.org (L.W.), wwei2@bidmc.harvard.edu (W.W.).

kinase activity. Our findings, therefore, uncover a layer of BRAF regulation and suggest p300 hyperactivation or *SIRT1* deficiency as potential biomarkers to determine ERK activation in melanomas.

Graphical Abstract
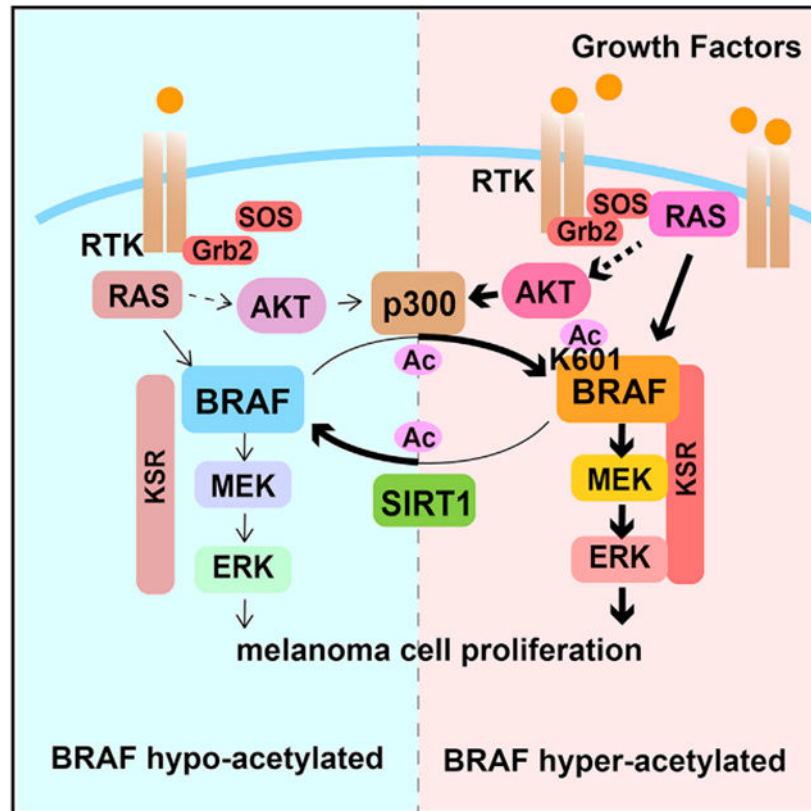
In brief

In tumor cells, hyperactivation of the BRAF protein kinase propels uncontrolled cell proliferation. BRAF hyperactivation is also achieved through several post-translational mechanisms. Dai et al. present an acetylation-dependent regulation of BRAF kinase function in melanoma cells, which serves to enhance BRAF oncogenic function and contributes to BRAF inhibitor resistance.

INTRODUCTION

The RAF family protein kinases A-Raf proto-oncogene (ARAF), B-Raf proto-oncogene (BRAF), and Raf-1 proto-oncogene (CRAF) play a vital role in regulating tumorigenesis primarily through activating its downstream MAPK/ERK kinase (MEK)/extracellular signal-regulated kinase (ERK) oncogenic signaling pathway (Wellbrock et al., 2004a). Activation of the RAF family of protein kinases involves multiple layers of protein post-translational modifications, as well as protein-protein interactions (McKay and Morrison, 2007). For example, RAS binding facilitates membrane localization of RAF proteins (Wellbrock et al., 2004a), whereas PP1- or PP2A-mediated dephosphorylation of RAF proteins disrupts

inhibitory 14-3-3 binding (Abraham et al., 2000; Jaumot and Hancock, 2001; Light et al., 2002). More importantly, phosphorylation at the activation segment facilitates the full activation of RAF kinases (Zhang and Guan, 2000). We have previously demonstrated that BRAF ubiquitination and degradation can be governed by the APC^{FZR1} ubiquitin E3 in normal melanocytes (Wan et al., 2017) and the ITCH ubiquitin E3 ligase in melanoma cells (Yin et al., 2019). However, whether BRAF activity and BRAF^{V600E} inhibitor sensitivity are regulated by additional post-translational modification remains poorly investigated.

Protein acetylation is a reversible post-translational modification catalyzed by the opposing activities of protein acetyltransferases and deacetylases (Glozak et al., 2005; Spange et al., 2009). p300 and CREB Binding Protein (CBP) are among the best studied histone acetyltransferases (HATs), which acetylate a large number of histones and non-histone proteins (Kimura et al., 2005). In addition to its well-characterized role in histone acetylation, p300 governs a wide spectrum of cellular functions through conjugating the acetyl group to its non-histone substrates. Known p300 non-histone substrates include the signal transducer and activator of transcription 3 (STAT3) (Wang et al., 2005; Yuan et al., 2005), nuclear factor κB (NF-κB) (Chen et al., 2001), and Yin Yang 1 (YY1) (Yao et al., 2001), as well as other cell fate regulatory proteins, such as Skp2 (Inuzuka et al., 2012) and AF4/FMR2 family member 1 (AFF1) (Kumari et al., 2019).

Here, we report that BRAF is subjected to p300-mediated acetylation at Lys601 (K601), which stimulates BRAF kinase activity. Moreover, we unveiled the deacetylase SIRT1 as the deacetylase antagonizing BRAF K601 acetylation. We found that K601 acetylation activates BRAF and facilitates melanomagenesis. Notably, the *BRAF*^{K601E} oncogenic mutation, which is frequently found in melanoma patients, could partially mimic K601 acetylation to facilitate BRAF activation. All these findings together uncover a previously undefined regulation of BRAF kinase activity and BRAF^{V600E} inhibitor resistance, thereby suggesting that ERK activation can be reflected partially by p300 hyperactivation or *SIRT1* deficiency in melanoma cells.

RESULTS

BRAF is acetylated by p300 at K601

A positive correlation between p300 and BRAF expression and their association with melanoma progression have been well documented (Bhandaru et al., 2014; Wang et al., 2018), which prompted us to investigate whether BRAF is directly modulated by p300. We found that endogenous BRAF was acetylated in both *BRAF*^{WT}-expressing HEK293 (Figure S1A) and *BRAF*^{V600E}-expressing A375 cells (Figure 1A). Among the five lysine acetyltransferases (Choudhary et al., 2014) examined, p300 was the major acetyltransferase to acetylate BRAF in cells (Figures 1B, S1B, and S1C). Furthermore, pharmacologically suppressing p300 by the selective p300 inhibitor A-485 (Lasko et al., 2017) abolished p300-mediated BRAF acetylation (Figure 1C). Unlike BRAF, neither ARAF nor CRAF was acetylated by p300 (Figure 1D). Moreover, p300-mediated acetylation occurred on both wild type (WT)- and V600E-BRAF (Figure 2E) and could be induced by insulin (Figure 1F), which activates p300 through the phosphatidylinositol 3-kinase (PI3K)/AKT signaling pathway (Huang and Chen, 2005).

In support of a direct acetylation of BRAF by p300, we observed that immunopurified BRAF proteins were acetylated by p300 *in vitro* (Figure 1G), and that BRAF interacted with p300 at both endogenous (Figure 1H) and exogenous (Figures 1I and S1D) levels. Notably, p300 specifically interacted with BRAF, but not ARAF or CRAF, when both RAF proteins and p300 were overexpressed in cells (Figure 1I). However, we found that endogenous ARAF and CRAF were also co-immunoprecipitated with p300 in 293T cells (Figure S1E), suggesting ARAF and CRAF might be pulled down by p300 through BRAF because RAF proteins form dimers (Figure S1F) (Brummer and McInnes, 2020). In support of this notion, when three RAF isoforms were ectopically expressed simultaneously, they were all pulled down by hemagglutinin (HA)-p300 (Figure S1G).

Next, we sought to determine the lysine residues in BRAF that are acetylated by p300. Mass spectrometry analysis revealed that five lysines in BRAF were acetylated by p300 in cells (Figures S1H and S1I). Mutating K418 and K601 to arginine largely abolished p300-mediated BRAF acetylation (Figures 1J, S1J, and S1K), suggesting that K418 and K601 are the major acetylation sites on BRAF. Given its localization in the activation segment of the BRAF kinase domain (Figure 1K) (Wan et al., 2004), K601 acetylation is expected to impose a more profound change on BRAF kinase activity compared to K418 acetylation. Indeed, using K-Q substitution to mimic lysine acetylation event (Inuzuka et al., 2012; Ye et al., 2017; Zaini et al., 2018), we found that K601Q-BRAF, but not K418Q-BRAF, augmented BRAF kinase activity in cells (Figure S1L), suggesting a positive regulation of BRAF kinase activity by p300-mediated acetylation. Furthermore, we found that depletion of *p300* led to decreased phos- phorylated (p) ERK in cells (Figure S1M), and ectopically expressing p300 increased pERK and pMEK in cells (Figures S1N and S1O). Given the more important role of K601 acetylation in modulating BRAF kinase activity, the K601 acetylation will be our major focus in the remainder of the study.

SIRT1 interacts with and deacetylates BRAF to attenuate BRAF/MEK/ERK signaling activity

We next sought to identify the deacetylase that functions as an "eraser" to remove the acetyl functional group from the modified K601; we found that nicotinamide (NAM) treatment resulted in a higher level of BRAF acetylation than trichostatin A (TSA) (Figure S2A). This indicated that sirtuin family deacetylases could be the deacetylases for BRAF. Indeed, we found that SIRT1 and SIRT6 bound stronger to BRAF (Figure 2A). Intriguingly, only SIRT1, but not SIRT6, could efficiently deacetylate BRAF (Figure 2B), indicating SIRT1 as the major deacetylase for BRAF in cells. In support of this, we found that compared to WTSIRT1, enzymatically deficient H363Y-SIRT1 (Armstrong et al., 2002) failed to deacetylate BRAF (Figure 2C). Furthermore, depletion of endogenous *SIRT1* in immortalized human primary melanocytes (IHPMs) (Garraway et al., 2005), HBL, and HEK293 cells led to the activation of the MEK/ERK signaling pathway (Figures 2D, S2B, and S2C), which could be rescued by WT-, but not the catalytically inactive H363Y-SIRT1 (Figure 2E). Likewise, compared to control mouse embryonic fibroblasts (MEFs) and A375 cells, pMEK and pERK levels were upregulated in *Sirt1$^{-/-}$* MEFs and sh*SIRT1*-A375 cells, respectively (Figures 2F-2H, S2D, and S2E), which might be caused by enhanced BRAF acetylation (Figures 2G and 2H). In contrast, ectopic expression of SIRT1 in *Sirt1$^{-/-}$* MEFs led to relatively compromised MEK/ERK signaling upon EGF treatment (Figure 2I).

Given the pivotal role of the MEK-ERK pathway in promoting cell proliferation, $Sirt1^{-/-}$ MEFs were more proliferative compared to WT MEFs (Figures 2J and 2K). Moreover, depletion of endogenous *SIRT1* in HBL cells facilitated *in vivo* xenograft tumor growth in a BRAF-dependent manner (Figures 2L-2N and S2F-S2H). In accordance, depletion of *p300* in HBL cells led to a marked decrease in colony formation (Figure S2I) and cell proliferation (Figures S2J and S2K). Together, these results revealed an important post-translational modification for BRAF mediated by p300 and SIRT1 at the K601 site that could facilitate BRAF oncogenic function.

Acetylation of K601 stimulates BRAF kinase activity and facilitates melanoma tumorigenesis

To further understand the importance of p300-mediated acetylation in BRAF kinase activity, we generated K601Q acetylation mutant to mimic the acetylation on K601 (Inuzuka et al., 2012). It is noteworthy that K601 has been found to be mutated in melanoma patients to glutamic acid (E) (Figure S3A) (Davies et al., 2002), suggesting that altering K601, either by mutation or through post-translational modifications such as acetylation, could activate BRAF. Notably, we found that compared to WT- and K601R-BRAF, V600E-, K601Q-, or K601E-BRAF is more potent in stimulating pMEK and pERK levels in cells (Figures 3A, 3B, and S3B-S3D). Consistently, compared to WT or K601R-BRAF, V600E-, K601Q-, and K601E-BRAF are more active to phosphorylate recombinant glutathione-S-transferase (GST-MEK1) *in vitro* (Figure 3C). To further determine whether acetylation-mediated BRAF activation is primarily through K601, we found that although overexpressing p300 or depleting *SIRT1* facilitates MEK and ERK activation in WT-BRAF-expressing cells, it failed to activate MEK/ERK in K601R-BRAF-expressing cells (Figures 3D and S3E). Likewise, ectopic overexpression of SIRT1 inhibited MEK/ERK in WT-BRAF-expressing, but not K601R-BRAF-expressing, cells (Figure 3E). Moreover, p300 overexpression accelerated cell proliferation in WT-BRAF-expressing, but not K601R-BRAF-expressing, HEK293 cells (Figure S3F).

V600E-BRAF drives melanocyte transformation and melanomagenesis (Wellbrock et al., 2004b). To determine whether K601Q, which mimics K601 acetylation, could promote melanomagenesis analogous to the oncogenic K601E-BRAF, we utilized a previously reported *in vitro* melanomagenesis model (Oba-Shinjo et al., 2006). Intriguingly, compared to WT-BRAF, V600E-, K601Q-, and K601E-BRAF were relatively more potent to activate MEK/ERK (Figure S3G) in melan-a cells, subsequently leading to increased cell proliferation (Figure S3H). Similarly, compared to WT-BRAF-expressing cells, expression of K601Q- or K601E-BRAF in B16 cells accelerated anchorage-in-dependent growth (Figures S3I and S3J). Moreover, compared to WT-BRAF, K601Q-BRAF promoted the growth of B16 tumor xenografts in nude mice (Figures 3F-3I and S3K).

Acetylation of BRAF-K601 modulates the interaction between BRAF and its binding partners

Recently resolved crystal structures of the BRAF kinase domain revealed that K601 exhibits side-chain flexibility, indicating that acetylation of K601 might cause a dramatic conformation change to the activation segment and thereby activate BRAF (Figures S3L and

S3M) (Grasso et al., 2016; Nishiguchi et al., 2017). Apart from a direct change of BRAF conformation, the activity of the BRAF/MEK/ERK kinase cascade is also governed by the interaction of BRAF with its binding partners (McKay and Morrison, 2007), which includes upstream RAS family proteins, downstream MEK kinases, the scaffolding protein KSR1, and the RAF inhibitor RKIP (Haling et al., 2014), as well as the dimeric interaction between two RAF molecules (Poulikakos and Rosen, 2011). Intriguingly, we found that compared to WT-BRAF, K601Q- and K601E-BRAF displayed increased binding with KSR1 (Figure 3J), enhanced dimerization with BRAF (Figure 3K) and CRAF (Figure 3L), and reduced interaction with the RAF inhibitor RKIP (Figure 3M). In accordance, ectopic expression of p300 enhanced the interaction of KSR1 with WT-, but not K601R-BRAF (Figures 3N and 3O). p300 ectopic expression also facilitated the dimerization of WT-, but not K601R-BRAF (Figures S3N and S3O). In contrast, expression of SIRT1 suppressed the binding between BRAF and KSR1 (Figure S3P). These results offer the molecular basis underlying the observation that acetylated BRAF species possess higher potency in activating downstream signals (Figure S3Q).

Notably, compared to WT-BRAF, the interaction between K601Q- or K601E-BRAF and its upstream activator NRAS (Figures S3R and S3S), but not KRAS (Figure S3T), was decreased. These results indicate that similar to V600E-BRAF, acetylated BRAF has a higher basal activity independent of upstream signals (Yao et al., 2015). In further support of this, we found that MEK1 was also disassociated from the active mutants of V600E-, K601Q-, and K601E-BRAF in contrast to WT-BRAF (Figures S3U and S3V). This finding is consistent with a previously described mechanism that constitutively active kinase does not require a constant binding with its substrate upon activation (Haling et al., 2014). Although the K601E- and K601Q-BRAF exhibited enhanced kinase activity *in vitro* (Figure 3C), acetylated BRAF proteins by pre-incubating with p300 (Figure 1G) did not exhibit a higher activity compared to non-treated BRAF (Figure S3W). Given the relatively small portion of BRAF protein that could be acetylated by p300 *in vitro* and in cells, this observation further supports the importance of K601 acetylation in modulating the BRAF/ MEK1/KSR1 signalosome assembly in addition to its role in directly changing the BRAF protein conformation. Together, these results demonstrate that acetylation of BRAF at K601 could activate the BRAF/MEK/ERK signaling cascade via rewiring the modules assembly of this pathway (Figure S3Q).

BRAF K601 acetylation contributes to the resistance of BRAF^{V600E} melanoma cells to vemurafenib

Acquired resistance to specific BRAF^{V600E} inhibitors is often observed in relapsed tumors after treatment (Poulikakos and Rosen, 2011). Despite exhibiting a similar activity to V600E-BRAF, consistent with a previous report (Menzies and Long, 2014), K601Q- and K601E-BRAF were insensitive to the BRAF^{V600E}-specific inhibitor vemurafenib (PLX4032) (Figures 4A, S4A, and S4B). In agreement with this finding, we found that the WM3130 and the YUQUEST melanoma cell lines harboring *BRAF*^{K601E} and *BRAF*^{K601N}, respectively (Smalley et al., 2008), were refractory to PLX4032 treatment (Figures 4B, 4C, and S4C). Moreover, depletion of *SIRT1* in BRAF^{V600E}-expressing A375 cells led to a marked resistance to PLX4032-mediated suppression of MEK/ERK activity (Figure

4D). Furthermore, HEK293 and B16 cells expressing BRAF V600E + K601E or V600E + K601Q exhibited marked resistance to PLX4032 (Figures 4E and 4F). Furthermore, compared to V600E-BRAF, B16 cells expressing V600E + K601Q-BRAF were relatively more resistant to PLX4032 *in vivo* (Figures 4G-4I).

Next, we examined whether inhibiting p300 modulates the sensitivity of melanoma cells to PLX4032. In *BRAF*^{V600E}-expressing A375 cells, combined treatment with a p300 inhibitor (C646) and PLX4032 led to a significant reduction in cell proliferation (Figures S4D and S4E), colony formation (Figures S4F and S4G), and cell viability (Figure S4H), and such loss of cell fitness may be partially caused by the reduction of the BRAF/MEK/ERK pathway activity (Figure S4I). C646-mediated sensitization of *BRAF*^{V600E} melanoma cells to PLX4032 treatment could also be observed in SK-MEL-256 and 888-MEL cells (Figures S4J and S4K). Moreover, inhibition of p300 by C646 sensitized V600E-BRAF-expressing, but not V600E + K601E-BRAF-expressing, HEK293 cells to PLX4032 (Figures S4L and S4M), suggesting an important role of K601 acetylation in mediating PLX4032 resistance in *BRAF*^{V600E} melanoma cells. Moreover, we found that co-treatment of PLX4032 with a SIRT1 activator, Resveratrol (Haigis and Sinclair, 2010), displayed a similar effect as the p300 inhibitor in suppressing the cell viability (Figures S4N-S4P), which was accompanied by reduced BRAF/MEK/ERK activity (Figure S4Q). Intriguingly, compared to V600E-BRAF-expressing cells, which were more resistant to PLX4032 when *SIRT1* was depleted (Figure S4R), loss of *SIRT1* in V600E + K601Q– and V600E + K601R-BRAF-expressing cells showed only a slight increase of PLX4032 resistance (Figure S4R). This result was further supported by the ectopic expression of SIRT1 in combination with PLX4032 treatment, where SIRT1 expression moderately sensitized V600E-BRAF-expressing, but not V600E + K601Q-expressing, cells to PLX4032 treatment (Figures S4S and S4T).

DISCUSSION

BRAF acetylation controlled by p300 and SIRT1 complements the multi-layered regulation of BRAF function

Aberrant activation of the BRAF kinase is achieved by a variety of mechanisms (Lavoie and Therrien, 2015; Yin et al., 2019). We present here a positive regulation of BRAF kinase activity by p300-mediated acetylation of BRAF at K601 (Figures 1J and 1K), which promotes melanoma cell growth (Figures 3F-3I). In addition to a direct impact of K601 acetylation on the conformation of BRAF catalytic center, our findings revealed an altered affinity of K601Q-BRAF or K601E-BRAF to KSR1 (Figure 3J), BRAF (Figure 3K), CRAF (Figure 3L), and RKIP(Figure 3M).These results provide molecular insights into the mechanism by which acetylated BRAF exhibits increased kinase activity in melanoma cells (Figure S3Q).

SIRT1 exhibits critical roles in multiple cellular functions, including apoptotic and stress responses, tumor suppression, inflammation, and longevity via its deacetylase activity (Baur et al., 2006; Michan and Sinclair, 2007). However, the function of SIRT1 in melanoma cells remains controversial and appears to be context dependent (Meliso et al., 2017; Sun et al., 2018; Wilking-Busch et al., 2018). Our findings favor a model in which SIRT1 plays a

tumor suppressor role in antagonizing BRAF K601 acetylation, thereby inhibiting BRAF oncogenic activity.

Acetylation of BRAF at K601 likely mimics the K601E oncogenic mutation

It is noteworthy that melanoma patients with *BRAF* K601E mutation failed to respond to dabrafenib treatment (Moiseyenko et al., 2019; Voskoboynik et al., 2016). Consistently, studies using melanoma cell lines harboring $BRAF^{K601E}$ demonstrate that compared to $BRAF^{V600E}$ melanoma cells, $BRAF^{K601E}$ cells are refractory to BRAF-V600E inhibitors (Yang et al., 2010). Moreover, in a preclinical study using a $BRAF^{K601E}$ patient-derived melanoma xenograft model, dabrafenib plus trametinib exhibited improved anti-tumor efficacy compared to trametinib alone (Rogiers et al., 2019). A recent report identified melanoma patients carrying a rare V600E2;K601I BRAF alteration (Consoli et al., 2020). Therefore, it is of great interest to further investigate how these patients respond to BRAF and/or MEK inhibition. Given the potential interplay between these two adjacent residues V600 and K601 at the center of the BRAF catalytic core, our findings suggest that K601 acetylation status could be used as a biomarker in anti-BRAF therapies to better guide the combinational treatment targeting upstream signals of the K601 acetylation.

Limitations of the study

Challenges in faithfully mimicking the K601 acetylation on the BRAF^V600E background

—Although it is widely utilized to mimic acetylation by substituting the lysine residue with glutamine (KQ), the KQ substitution may exhibit different function(s) compared to lysine acetylation (Fujimoto et al., 2012). Lysine acetylation modulates protein function primarily through two mechanisms. It neutralizes the basic charge of the lysine side chain, thereby disabling the ɛ-amino group-mediated protein functions. Lysine acetylation also places an acetyl group on the lysine side chain, which could be recognized by acetyl group reader proteins (Kamieniarz and Schneider, 2009). It is apparent that the KQ substitution is capable of mimicking only the loss of function caused by lysine acetylation. Hence further profiling of the interactome of affinity-purified, acetylated BRAF will likely be crucial to fully understand the underlying mechanism(s) of how acetylation of BRAF-K601 augments its kinase activity in cells.

Notably, the K601 residue sits in the center of the BRAF "activation loop" consisting of the key amino acids (T599-S602) that dictate BRAF kinase activity. A slight modification of the side-chain composition has been suggested to impact substantially on BRAF kinase activity and/or RAF dimerization status (Park et al., 2019). In this regard, although K601R serves well as a non-acetylable mimetic, in cells it might also cause a slight disposition of the BRAF polypeptide chain at the "activation loop," which could paradoxically alter the PLX4032 response. Therefore, future development of a highly specific K601-Ac antibody could help us further monitor the change of K601 acetylation status when exposing $BRAF^{V600E}$ melanoma cells to vemurafenib.

Part of our results were obtained using the HEK293 cell line to compare the activity of different BRAF mutants. To assess the impact of K601 acetylation in a more physiological setting, the development of CRISPR-Cas9-edited K601Q and K601R melanoma cell lines is

an imminent need to extend this present study. Moreover, besides colony formation assays, *in vivo* animal studies such as xenografted assays should be performed to evaluate the effects of BRAF-K601 acetylation event and *SIRT1* knockdown in tumorigenesis *in vivo*.

STAR★METHODS

RESOURCE AVAILABILITY

Lead contact—Further information and requests for resources and reagents should be directed to and will be fulfilled by the Lead Contact, Wenyi Wei (wwei2@bidmc.harvard.edu).

Materials availability—Plasmids generated in this study is available upon request and will be shared without restriction.

Data and code availability—Original Western blot images have been deposited at Mendeley and are publicly available as of the date of publication. The DOI is listed in the key resources table. This paper does not report original code. Any additional information required to reanalyze the data reported in this paper is available from the lead contact upon request.

EXPERIMENTAL MODEL AND SUBJECT DETAILS

Cell lines—HEK293, HEK293T, MEFs, HBL (Zimmerer et al., 2013), A375, B16, SK-MEL-256, 888-MEL and WM3130 were cultured in DMEM medium supplemented with 10% FBS, 100 Units of penicillin and 100 mg/mL streptomycin. YUQUEST cells, which are kind gift from Dr. Ruth Halaban in Yale University, were cultured in OPTI-MEM medium supplemented with 5% FBS, 100 Units of penicillin and 100 mg/mL streptomycin. $Sirt1^{+/+}$ and $Sirt1^{-/-}$ MEFs was kindly gifted by Dr. Kunping Lu in Harvard Medical School. Cell culture conditions for human primary melanocytes (HPM), mouse primary melanocytes (melan-a) and hTERT/p53DD/R24C-Cdk4 immortalized human melanocytes (IHPM) have been described previously (Cao et al., 2013).

Mice—Nude mice (NCRNU-M-M, 5–6 weeks of age, female) were purchased from Taconic (http://www.taconic.com/). All care was taken, and experimental procedures were conducted according to Beth Israel Deaconess Medical Center Institutional Animal Care and Use Committee protocol (#019–2021).

METHOD DETAILS

Plasmids—The detailed information of used plasmids is listed on the key resources table. BRAF WT and V600E cDNAs were subcloned into pcDNA3-HA and pFlag-CMV vectors. pBabe-puro-BRAF and pBabe-puro-BRAF^{V600E} were obtained from Dr. William Hahn (Boehm et al., 2007). PGEX-4T-1-NRas, PGEX-4T-1-MEK1, pLenti-BRAF-WT, V600E, K601Q, K601E, K601R, V600E + K601Q and V600E + K601E were subcloned into indicated vectors. The QuikChange XL Site-Directed Mutagenesis Kit (Stratagene) was used to generate various BRAF mutants according to the manufacturer's instructions. More

details of plasmid constructions are available upon request. shRNAs against BRAF, p300 and SIRT1 were purchased from OpenBiosystems.

Antibodies—The detailed information of used antibodies is listed in the key resources table. All primary antibodies were used at 1:1000–2000 dilution in TBST buffer with 5% non-fat milk for Western blot. The secondary antibodies were used at a 1:3000 dilution in TBST buffer with 5% non-fat milk.

Immunoblots and immunoprecipitation—Cells were lysed in EBC buffer (50 mM Tris pH 7.5, 120 mM NaCl, 0.5% NP-40) supplemented with protease inhibitors (Complete Mini, Roche) and phosphatase inhibitors (phosphatase inhibitor cocktail set I and II, Calbiochem). The protein concentrations of the lysates were measured using the Bio-Rad protein assay reagent on a Beckman Coulter DU-800 spectrophotometer. Equal amounts of cell lysates were then resolved by SDS-PAGE and immunoblotted with indicated antibodies. For immunoprecipitation analysis, 1000 μg lysates were incubated with the appropriate antibody (1–2 μg) for 3–4 h at 4°C followed by 1 h incubation with Protein A Sepharose beads (GE Healthcare). The immuno-complexes were washed five times with NETN buffer (20 mM Tris, pH 8.0, 100 mM NaCl, 1 mM EDTA and 0.5% NP-40) before being resolved by SDS-PAGE and immunoblotted with indicated antibodies.

***In vitro* binding assay**—The *in vitro* binding to immobilized GST proteins was performed according to the protocol described previously (Gao et al., 2009; Wei et al., 2004).

***In vitro* kinase assay**—The BRAF *in vitro* kinase assays were performed as previously described (Zhang and Guan, 2000). Briefly, BRAF was immunopurified using Flag M2 antibody and lysates from 293T cells transfected with indicated Flag-BRAF constructs. Flag-BRAF were eluted using 3X FLAG Peptide (Sigma). GST-MEK1 was expressed in BL21 *E.coli* cells and purified using Glutathione Sepharose 4B Media (GE Healthcare Life Sciences) according to the manufacturer's instructions. BRAF kinase was incubated with 0.2 μg of GST-MEK1 in kinase assay buffer (10 mM HEPES pH 8.0, 10 mM MgCl$_2$, 1 mM dithiothreitol, 0.1 mM ATP) in a volume of 30 μL for 15 min at 30°C followed by the addition of SDS-PAGE loading sample buffer to stop the reaction before being resolved by SDS-PAGE.

***In vitro* acetyltransferase assay**—p300 *in vitro* acetyltransferase assay was conducted as previously described (Balasubramanyam et al., 2003). Briefly, immunopurified and eluted Flag-BRAF proteins were incubated with immunopurified HA-p300 protein in histone acetyltransferase buffer (50 mM Tris-HCl pH 8.0, 10% (v/v) glycerol, 1 mM dithiothreitol, 0.1 mM EDTA, 10 mM butyric acid and 100 μM acetyl-CoA)at 30°C for 60 min.

Cell transfection and viral infection—The transient transfection was done by Lipofactimine and Plus reagent as previously described (Wan et al., 2011). Packaging of lentiviral shRNA or cDNA expressing virus as well as subsequent infection of various cell lines were performed according to the protocol described previously (Boehm et al., 2005).

Cell viability assays—The indicated cell lines were seeded in 96-well (3×10^3 cells/well) plates and cultured in 100 μL medium containing 10% serum. After 24 h, cells were treated with or without various concentrations of compounds in 50 μL medium for 48 h and the cell viability was measured using the CellTiterGlo (Promega) according to the manufacturer's instructions.

Cell proliferation assays—Cells were seeded in 6-well plates (1×10^5–2×10^5 cells/ well) in the medium. At the indicated time points, the cells were trypsinized and cell number was counted under the microscope.

Mass spectrometry analysis—For mass spectrometry analysis, 10 cm dishes of 293T cells were transfected with Flag-BRAF and HA-p300. 30 h post-transfection, 293T cells were treated with 1 μM trichostatin A (TSA) and 10 mM nicotinamide (NAM) for 10 h to block the histone deacetylases (HDAC) activity. The anti-Flag immunoprecipitations (IP) were performed with the whole cell lysates derived from the 293T cells in the presence of 2 μM TSA and 10 mM NAM. The immunoprecipitate was resolved by SDS-PAGE and acetylation was detected by mass spectrum analysis. In gel digestion and reversed phase microcapillary/tandem mass spectrometry (LC-MS/MS) were performed as described previously (Inuzuka et al., 2010; Tang et al., 2007).

Colony formation and soft agar assays—For the short-term colony formation assay, the indicated cells were seeded in 6-well plates (1000–3000 cells/well) in medium and cultured for one to two weeks dependent on the size of the colony. Then the cells were fixed by 10% methanol and 10% acetic acid, stained with crystal violet and counted. For the long-term soft agar assay, 2% melting Nobel agar was mixed with culture medium to make the 0.4% and 0.8% agar and stored at 50°C. 2 mL 0.8% Nobel agar was added on the bottom of the 6-well plate. 1×10^4 or 3×10^4 cells per well were mixed with 2 mL 0.4% agar and was added on top of previously added 0.8% agar. After routine culture for 3 weeks-5 weeks, colony numbers were stained with iodonitrotetrazolium chloride (1 mg/mL) (sigma I10406) and counted.

Mouse xenograft assay—Mouse xenograft assays were performed as described previously (Liu et al., 2014). Briefly, 1×10^5-1×10^6 indicated cells were injected into the flank of nude mice (NCRNU-M-M from Taconic, 5–6 weeks of age, female). At the indicated time points, tumor size was measured with a caliper, and the tumor volume was determined with the formula: $L \times W^2 \times 0.5$, where L is the longest diameter and W is the shortest diameter. After the tumor grew big enough, mice were sacrificed and the solid tumors were dissected, and then tumor weights were measured and recorded post-necropsy.

Ethics statement—All experimental procedures were approved by the Institutional Animal Care & Use Committee (IACUC, RN150D) at Beth Israel Deaconess Medical Center with protocol #043–2015. The research projects that are approved by the IACUC are operated according to the applicable institutional regulations. The institute is committed to the highest ethical standards of care for animals used for continued progress in the field of human cancer research.

Author Manuscript

Author Manuscript

Author Manuscript

Author Manuscript

QUANTIFICATION AND STATISTICAL ANALYSIS

All quantitative data were shown as the mean ± S.E.M. or the mean ± S.D. as indicated by at least three independent experiments or technical replicates. Differences between groups were evaluated by SPSS One-way ANOVA following by Student's t test. $p < 0.05$ was considered statistically significant.

Supplementary Material

Refer to Web version on PubMed Central for supplementary material.

ACKNOWLEDGMENTS

REFERENCES

Abraham D, Podar K, Pacher M, Kubicek M, Welzel N, Hemmings BA, Dilworth SM, Mischak H, Kolch W, and Baccarini M (2000). Raf-1-associated protein phosphatase 2A as a positive regulator of kinase activation. J. Biol. Chem 275, 22300–22304. [PubMed: 10801873]

Armstrong CM, Kaeberlein M, Imai SI, and Guarente L (2002). Mutations in Saccharomyces cerevisiae gene SIR2 can have differential effects on in vivo silencing phenotypes and in vitro histone deacetylation activity. Mol. Biol. Cell 13, 1427–1438. [PubMed: 11950950]

Balasubramanyam K, Swaminathan V, Ranganathan A, and Kundu TK (2003). Small molecule modulators of histone acetyltransferase p300. J. Biol. Chem 278, 19134–19140. [PubMed: 12624111]

Baur JA, Pearson KJ, Price NL, Jamieson HA, Lerin C, Kalra A, Prabhu VV, Allard JS, Lopez-Lluch G, Lewis K, et al. (2006). Resveratrol improves health and survival of mice on a high-calorie diet. Nature 444, 337–342. [PubMed: 17086191]

Bhandaru M, Ardekani GS, Zhang G, Martinka M, McElwee KJ, Li G, and Rotte A (2014). A combination of p300 and Braf expression in the diagnosis and prognosis of melanoma. BMC Cancer 14, 398. [PubMed: 24893747]

Boehm JS, Hession MT, Bulmer SE, and Hahn WC (2005). Transformation of human and murine fibroblasts without viral oncoproteins. Mol. Cell. Biol 25, 6464–6474. [PubMed: 16024784]

Boehm JS, Zhao JJ, Yao J, Kim SY, Firestein R, Dunn IF, Sjostrom SK, Garraway LA, Weremowicz S, Richardson AL, et al. (2007). Integrative genomic approaches identify IKBKE as a breast cancer oncogene. Cell 129, 1065–1079. [PubMed: 17574021]

Brummer T, and McInnes C (2020). RAF kinase dimerization: implications for drug discovery and clinical outcomes. Oncogene 39, 4155–4169. [PubMed: 32269299]

Cao J, Wan L, Hacker E, Dai X, Lenna S, Jimenez-Cervantes C, Wang Y, Leslie NR, Xu GX, Widlund HR, et al. (2013). MC1R is a potent regulator of PTEN after UV exposure in melanocytes. Mol. Cell 51, 409–422. [PubMed: 23973372]

Chen L, Fischle W, Verdin E, and Greene WC (2001). Duration of nuclear NF-kappaB action regulated by reversible acetylation. Science 293, 1653–1657. [PubMed: 11533489]

Choudhary C, Weinert BT, Nishida Y, Verdin E, and Mann M (2014). The growing landscape of lysine acetylation links metabolism and cell signalling. Nat. Rev. Mol. Cell Biol 15, 536–550. [PubMed: 25053359]

Consoli F, Barbieri G, Picciolini M, Medicina D, Bugatti M, Tovazzi V, Liserre B, Zambelli C, Zorzi F, Berruti A, et al. (2020). A rare complex BRAF mutation involving codon V600 and K601 in primary cutaneous melanoma: case report. Front. Oncol 10, 1056. [PubMed: 32754440]

Davies H, Bignell GR, Cox C, Stephens P, Edkins S, Clegg S, Teague J, Woffendin H, Garnett MJ, Bottomley W, et al. (2002). Mutations of the BRAF gene in human cancer. Nature 417, 949–954. [PubMed: 12068308]

Fujimoto H, Higuchi M, Koike M, Ode H, Pinak M, Bunta JK, Nemoto T, Sakudoh T, Honda N, Maekawa H, et al. (2012). A possible overestimation of the effect of acetylation on lysine residues in KQ mutant analysis. J. Comput. Chem 33, 239–246. [PubMed: 22072565]

Gao D, Inuzuka H, Korenjak M, Tseng A, Wu T, Wan L, Kirschner M, Dyson N, and Wei W (2009). Cdh1 regulates cell cycle through modulating the claspin/Chk1 and the Rb/E2F1 pathways. Mol. Biol. Cel 20, 3305–3316.

Garraway LA, Widlund HR, Rubin MA, Getz G, Berger AJ, Ramaswamy S, Beroukhim R, Milner DA, Granter SR, Du J, et al. (2005). Integrative genomic analyses identify MITF as a lineage survival oncogene amplified in malignant melanoma. Nature 436, 117–122. [PubMed: 16001072]

Glozak MA, Sengupta N, Zhang X, and Seto E (2005). Acetylation and deacetylation of non-histone proteins. Gene 363, 15–23. [PubMed: 16289629]

Grasso M, Estrada MA, Ventocilla C, Samanta M, Maksimoska J, Villanueva J, Winkler JD, and Marmorstein R (2016). Chemically linked vemurafenib inhibitors promote an inactive BRAF(V600E) conformation. ACS Chem. Biol 11, 2876–2888. [PubMed: 27571413]

Haigis MC, and Sinclair DA (2010). Mammalian sirtuins: biological insights and disease relevance. Annu. Rev. Pathol 5, 253–295. [PubMed: 20078221]

Haling JR, Sudhamsu J, Yen I, Sideris S, Sandoval W, Phung W, Bravo BJ, Giannetti AM, Peck A, Masselot A, et al. (2014). Structure of the BRAF-MEK complex reveals a kinase activity independent role for BRAF in MAPK signaling. Cancer Cell 26, 402–413. [PubMed: 25155755]

Huang WC, and Chen CC (2005). Akt phosphorylation of p300 at Ser-1834 is essential for its histone acetyltransferase and transcriptional activity. Mol. Cell Biol 25, 6592–6602. [PubMed: 16024795]

Inuzuka H, Gao D, Finley LW, Yang W, Wan L, Fukushima H, Chin YR, Zhai B, Shaik S, Lau AW, et al. (2012). Acetylation-dependent regulation of Skp2 function. Cell 150, 179–193. [PubMed: 22770219]

Inuzuka H, Tseng A, Gao D, Zhai B, Zhang Q, Shaik S, Wan L, Ang XL, Mock C, Yin H, et al. (2010). Phosphorylation by casein kinase I promotes the turnover of the Mdm2 oncoprotein via the SCF(beta-TRCP) ubiquitin ligase. Cancer Cell 18, 147–159. [PubMed: 20708156]

Jaumot M, and Hancock JF (2001). Protein phosphatases 1 and 2A promote Raf-1 activation by regulating 14-3-3 interactions. Oncogene 20, 3949–3958. [PubMed: 11494123]

Kamieniarz K, and Schneider R (2009). Tools to tackle protein acetylation. Chem. Biol 16, 1027–1029. [PubMed: 19875076]

Kimura A, Matsubara K, and Horikoshi M (2005). A decade of histone acetylation: marking eukaryotic chromosomes with specific codes. J. Biochem 138, 647–662. [PubMed: 16428293]

Kumari N, Hassan MA, Lu X, Roeder RG, and Biswas D (2019). AFF1 acetylation by p300 temporally inhibits transcription during genotoxic stress response. Proc. Natl. Acad. Sci. U S A 116, 22140–22151. [PubMed: 31611376]

Lasko LM, Jakob CG, Edalji RP, Qiu W, Montgomery D, Digiammarino EL, Hansen TM, Risi RM, Frey R, Manaves V, et al. (2017). Discovery of a selective catalytic p300/CBP inhibitor that targets lineage-specific tumours. Nature 550, 128–132. [PubMed: 28953875]

Lavoie H, and Therrien M (2015). Regulation of RAF protein kinases in ERK signalling. Nat. Rev. Mol. Cell Biol 16, 281–298. [PubMed: 25907612]

Light Y, Paterson H, and Marais R (2002). 14-3-3 antagonizes Ras-mediated Raf-1 recruitment to the plasma membrane to maintain signaling fidelity. Mol. Cell Biol 22, 4984–4996. [PubMed: 12077328]

Liu P, Begley M, Michowski W, Inuzuka H, Ginzberg M, Gao D, Tsou P, Gan W, Papa A, Kim BM, et al. (2014). Cell-cycle-regulated activation of Akt kinase by phosphorylation at its carboxyl terminus. Nature 508, 541–545. [PubMed: 24670654]

McKay MM, and Morrison DK (2007). Integrating signals from RTKs to ERK/MAPK. Oncogene 26, 3113–3121. [PubMed: 17496910]

Meliso FM, Micali D, Silva CT, Sabedot TS, Coetzee SG, Koch A, Fahlbusch FB, Noushmehr H, Schneider-Stock R, and Jasiulionis MG (2017). SIRT1 regulates Mxd1 during malignant melanoma progression. Oncotarget 8, 114540–114553. [PubMed: 29383100]

Menzies AM, and Long GV (2014). Dabrafenib and trametinib, alone and in combination for BRAF-mutant metastatic melanoma. Clin. Cancer Res 20, 2035–2043. [PubMed: 24583796]

Michan S, and Sinclair D (2007). Sirtuins in mammals: insights into their biological function. Biochem. J 404, 1–13. [PubMed: 17447894]

Moiseyenko FV, Egorenkov VV, Kramchaninov MM, Artemieva EV, Aleksakhina SN, Holmatov MM, Moiseyenko VM, and Imyanitov EN (2019). Lack of response to vemurafenib in melanoma carrying BRAF K601E mutation. Case Rep. Oncol 12, 339–343. [PubMed: 31182949]

Nihira NT, Ogura K, Shimizu K, North BJ, Zhang J, Gao D, Inuzuka H, and Wei W (2017). Acetylation-dependent regulation of MDM2 E3 ligase activity dictates its oncogenic function. Sci. Signal 10, 466.

Nishiguchi GA, Rico A, Tanner H, Aversa RJ, Taft BR, Subramanian S, Setti L, Burger MT, Wan L, Tamez V, et al. (2017). Design and discovery of N-(2-Methyl-5'-morpholino-6'-((tetrahydro-2H-pyran-4-yl)oxy)-[3,3'-bipyridin]-5-y l)-3-(trifluoromethyl)benzamide (RAF709): a potent, selective, and efficacious RAF inhibitor targeting RAS mutant cancers. J. Med. Chem 60, 4869–4881. [PubMed: 28557458]

Oba-Shinjo SM, Correa M, Ricca TI, Molognoni F, Pinhal MA, Neves IA, Marie SK, Sampaio LO, Nader HB, Chammas R, et al. (2006). Melanocyte transformation associated with substrate adhesion impediment. Neoplasia 8, 231–241. [PubMed: 16611417]

Park E, Rawson S, Li K, Kim BW, Ficarro SB, Pino GG, Sharif H, Marto JA, Jeon H, and Eck MJ (2019). Architecture of autoinhibited and active BRAF-MEK1-14-3-3 complexes. Nature 575, 545–550. [PubMed: 31581174]

Poulikakos PI, and Rosen N (2011). Mutant BRAF melanomas–dependence and resistance. Cancer Cell 19, 11–15. [PubMed: 21251612]

Rogiers A, Thomas D, Vander Borght S, van den Oord JJ, Bechter O, Dewaele M, Rambow F, Marine JC, and Wolter P (2019). Dabrafenib plus trametinib in BRAF K601E-mutant melanoma. Br. J. Dermatol 180, 421–422. [PubMed: 30248172]

Smalley KSM, Xiao M, Villanueva J, Nguyen TK, Flaherty KT, Letrero R, Van Belle P, Elder DE, Wang Y, Nathanson KL, et al. (2008). CRAF inhibition induces apoptosis in melanoma cells with non-V600E BRAF mutations. Oncogene 28, 85–94. [PubMed: 18794803]

Spange S, Wagner T, Heinzel T, and Kramer OH (2009). Acetylation of non-histone proteins modulates cellular signalling at multiple levels. Int. J. Biochem. Cell Biol 41, 185–198. [PubMed: 18804549]

Sun T, Jiao L, Wang Y, Yu Y, and Ming L (2018). SIRT1 induces epithelial-mesenchymal transition by promoting autophagic degradation of E-cadherin in melanoma cells. Cell Death Dis. 9, 136. [PubMed: 29374154]

Tang X, Gao JS, Guan YJ, McLane KE, Yuan ZL, Ramratnam B, and Chin YE (2007). Acetylation-dependent signal transduction for type I interferon receptor. Cell 131, 93–105. [PubMed: 17923090]

Voskoboynik M, Mar V, Mailer S, Colebatch A, Fennessy A, Logan A, Hewitt C, Cebon J, Kelly J, and McArthur G (2016). Clinicopathological characteristics associated with BRAF(K601E) and BRAF(L597) mutations in melanoma. Pigment Cel. Melanoma Res 29, 222–228.

Wan L, Chen M, Cao J, Dai X, Yin Q, Zhang J, Song SJ, Lu Y, Liu J, Inuzuka H, et al. (2017). The APC/C E3 ligase complex activator FZR1 restricts BRAF oncogenic function. Cancer Discov. 7, 424–441. [PubMed: 28174173]

Wan L, Zou W, Gao D, Inuzuka H, Fukushima H, Berg AH, Drapp R, Shaik S, Hu D, Lester C, et al. (2011). Cdh1 regulates osteoblast function through an APC/C-independent modulation of Smurf1. Mol. Cell 44, 721–733. [PubMed: 22152476]

Wan PT, Garnett MJ, Roe SM, Lee S, Niculescu-Duvaz D, Good VM, Jones CM, Marshall CJ, Springer CJ, Barford D, et al. (2004). Mechanism of activation of the RAF-ERK signaling pathway by oncogenic mutations of B-RAF. Cell 116, 855–867. [PubMed: 15035987]

Wang R, Cherukuri P, and Luo J (2005). Activation of Stat3 sequence-specific DNA binding and transcription by p300/CREB-binding protein-mediated acetylation. J. Biol. Chem 280, 11528–11534. [PubMed: 15649887]

Wang R, He Y, Robinson V, Yang Z, Hessler P, Lasko LM, Lu X, Bhathena A, Lai A, Uziel T, et al. (2018). Targeting lineage-specific MITF pathway in human melanoma cell lines by A-485, the selective small-molecule inhibitor of p300/CBP. Mol. Cancer Ther 17, 2543–2550. [PubMed: 30266801]

Wei W, Ayad NG, Wan Y, Zhang GJ, Kirschner MW, and Kaelin WG Jr. (2004). Degradation of the SCF component Skp2 in cell-cycle phase G1 by the anaphase-promoting complex. Nature 428, 194–198. [PubMed: 15014503]

Wellbrock C, Karasarides M, and Marais R (2004a). The RAF proteins take centre stage. Nat. Rev. Mol. Cell Biol 5, 875–885. [PubMed: 15520807]

Wellbrock C, Ogilvie L, Hedley D, Karasarides M, Martin J, Niculescu-Duvaz D, Springer CJ, and Marais R (2004b). V599EB-RAF is an oncogene in melanocytes. Cancer Res. 64, 2338–2342. [PubMed: 15059882]

Wilking-Busch MJ, Ndiaye MA, Liu X, and Ahmad N (2018). RNA interference-mediated knockdown of SIRT1 and/or SIRT2 in melanoma: identification of downstream targets by large-scale proteomics analysis. J. Proteomics 170, 99–109. [PubMed: 28882678]

Yang H, Higgins B, Kolinsky K, Packman K, Go Z, Iyer R, Kolis S, Zhao S, Lee R, Grippo JF, et al. (2010). RG7204 (PLX4032), a selective BRAFV600E inhibitor, displays potent antitumor activity in preclinical melanoma models. Cancer Res. 70, 5518–5527. [PubMed: 20551065]

Yao YL, Yang WM, and Seto E (2001). Regulation of transcription factor YY1 by acetylation and deacetylation. Mol. Cell. Biol 21, 5979–5991. [PubMed: 11486036]

Yao Z, Torres NM, Tao A, Gao Y, Luo L, Li Q, de Stanchina E, Abdel-Wahab O, Solit DB, Poulikakos PI, et al. (2015). BRAF mutants evade ERK-dependent feedback by different mechanisms that determine their sensitivity to pharmacologic inhibition. Cancer Cell 28, 370–383. [PubMed: 26343582]

Ye Q, Ji QQ, Yan W, Yang F, and Wang ED (2017). Acetylation of lysine-amino groups regulates aminoacyl-tRNA synthetase activity in Escherichia coli. J. Biol. Chem 292, 10709–10722. [PubMed: 28455447]

Yin Q, Han T, Fang B, Zhang G, Zhang C, Roberts ER, Izumi V, Zheng M, Jiang S, Yin X, et al. (2019). K27-linked ubiquitination of BRAF by ITCH engages cytokine response to maintain MEK-ERK signaling. Nat. Commun 10, 1870. [PubMed: 31015455]

Yuan ZL, Guan YJ, Chatterjee D, and Chin YE (2005). Stat3 dimerization regulated by reversible acetylation of a single lysine residue. Science 807, 269–273.

Zaini MA, Muller C, de Jong TV, Ackermann T, Hartleben G, Kortman G, Guhrs KH, Fusetti F, Kramer OH, Guryev V, et al. (2018). A p300 and SIRT1 regulated acetylation switch of C/EBPalpha controls mitochondrial function. Cell Rep. 22, 497–511. [PubMed: 29320743]

Zhang BH, and Guan KL (2000). Activation of B-Raf kinase requires phosphorylation of the conserved residues Thr598 and Ser601. EMBO J. 19, 5429–5439. [PubMed: 11032810]

Zimmerer RM, Korn P, Demougin P, Kampmann A, Kokemuller H, Eckardt AM, Gellrich NC, and Tavassol F (2013). Functional features of cancer stem cells in melanoma cell lines. Cancer Cell. Int 13, 78. [PubMed: 23915418]

Highlights

- p300 acetylates BRAF at K601 to promote BRAF kinase activity

- Deacetylation of BRAF by SIRT1 decreases BRAF kinase activity

- BRAF-K601 acetylation modulates the interaction of BRAF with its binding partners
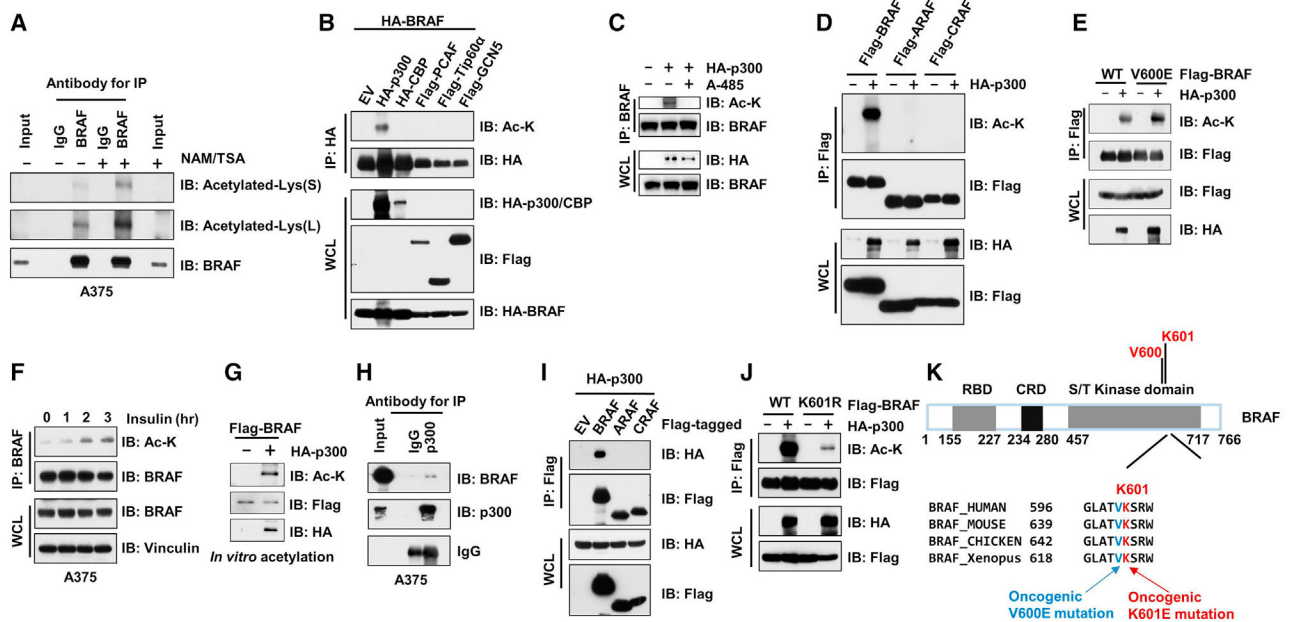
Figure 1. p300 specifically interacts with BRAF to promote acetylation of BRAF at K601

(A) Immunoblot (IB) analysis of whole-cell lysates (WCL) and anti-BRAF immunoprecipitates (IPs) derived from A375 cells. Cells were pretreated for 1 h with TSA (2 μM) and NAM (10 mM) before harvest.

(B) IB analysis of WCLs and anti-HA IPs derived from 293 cells transfected with the indicated constructs.

(C) IB analysis of WCLs and anti-BRAF IPs derived from 293 cells transfected with HA-p300 as indicated. 3 μM p300 inhibitor A-485 was added 12 h before the harvest as indicated. Cells were pretreated with TSA and NAM as described in (A).

(D and E) IB analysis of WCLs and anti-FLAG IPs derived from 293 cells transfected with the indicated constructs. Cells were pretreated with TSA and NAM as described in (A).

(F) IB analysis of WCLs derived from A375 and anti-BRAF IPs. Cells were serum starved for 24 h and then collected after 1 h following the addition of insulin. Cells were pretreated with TSA and NAM as described in (A).

(G) *In vitro* acetylation assay was conducted by incubating immunopurified and eluted FLAG-BRAF proteins with immunopurified HA-p300 proteins in acetyltransferase assay buffer at 30°C for 60 min.

(H) IB analysis of A375 WCLs and anti-p300 IPs. Rabbit IgG was used as a negative control for the IPs.

(I and J) IB analysis of WCLs and anti-FLAG IPs derived from 293 cells transfected with the indicated constructs.

(K) Sequence alignment of the putative K601 acetylation site in BRAF from different species.

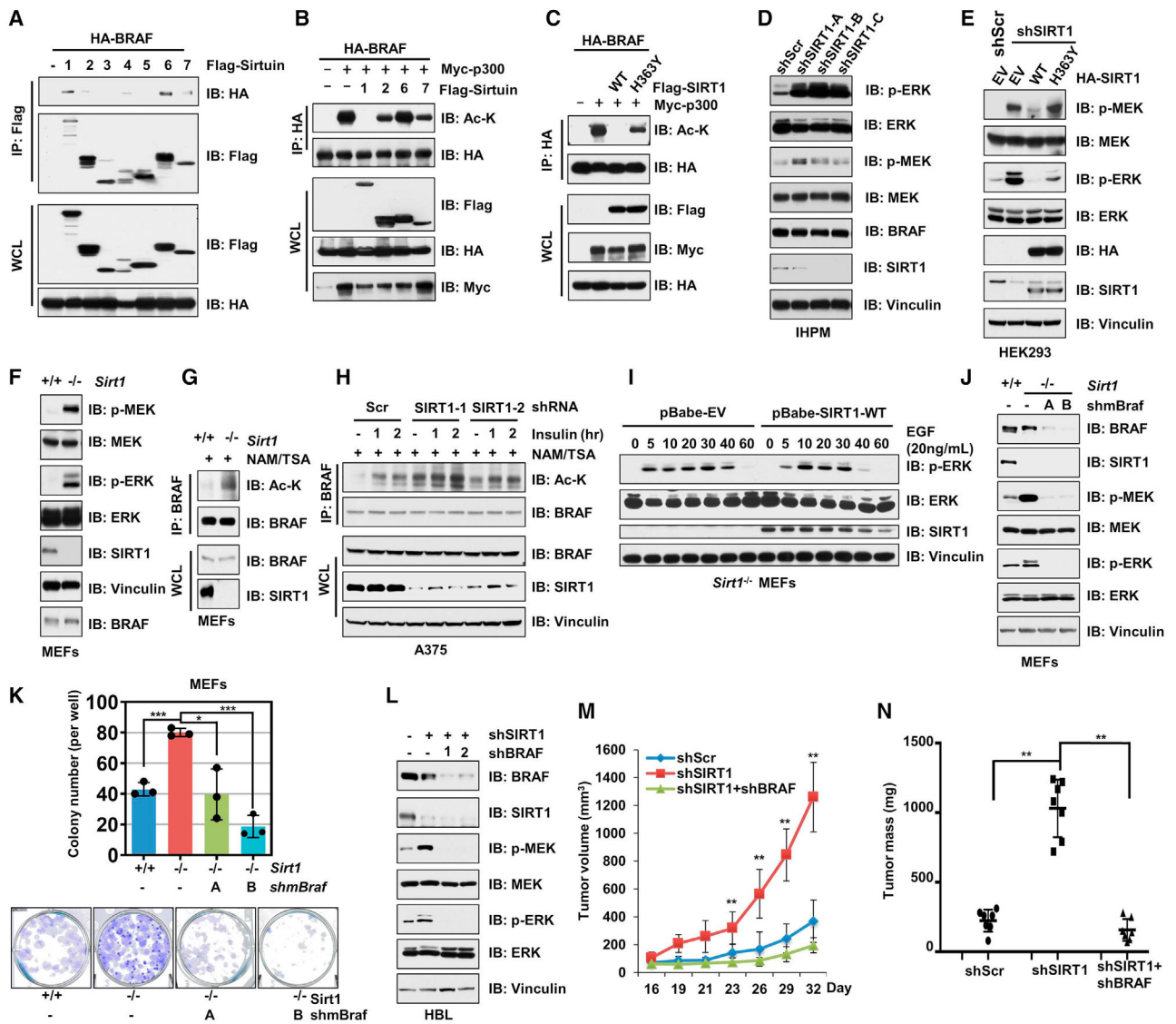Ac-K, acetylated-Lys. See also Figure S1.

Figure 2. SIRT1 is a deacetylase to antagonize BRAF-K601 acetylation

(A) Immunoblot (IB) analysis of whole-cell lysates (WCLs) and anti-FLAG immunoprecipitates (IPs) derived from 293 cells transfected with HA-BRAF and the indicated FLAG-Sirtuin constructs.

(B and C) IB analysis of WCLs and anti-HA IPs derived from 293 cells transfected with HA-BRAF, Myc-p300, and the indicated FLAG-Sirtuin (B) or FLAG-SIRT1 (C) constructs.

(D) IB analysis of WCLs derived from immortalized human melanocytes (IHPM) infected with shScr (as the negative control) or the indicated lentiviral sh*SIRT1* constructs. The infected cells were selected with 1 μg/mL puromycin for 72 h before harvest.

(E) IB analysis of WCLs derived from the sh*SIRT1*-infected 293 cells transfected with the indicated SIRT1 constructs.

(F) IB analysis of WCLs derived from the *Sirt1*^+/+ and *Sirt1*^−/− MEFs.

(G) IB analysis of WCLs and anti-BRAF IPs derived from *Sirt1*^+/+ and *Sirt1*^−/− MEFs. Cells were pretreated for 1 h with TSA (2 μM) and NAM (10 mM) before harvest.

(H) IB analysis of WCLs and anti-BRAF IPs derived from sh*SIRT1*-infected A375 cells. Cells were serum starved for 24 h and then collected after 1–2 h following the addition of insulin. Cells were pretreated with TSA and NAM as described in (E).

(I and J) IB analysis of WCLs derived from *Sirt1*$^{-/-}$ MEFs infected with the indicated retroviral constructs (I) or the indicated lentiviral short hairpin RNA targeting BRAF (shBRAF) constructs (J).

(K) Colony formation assays of *Sirt1*$^{+/+}$ and *Sirt1*$^{-/-}$ MEFs with depletion of *Braf*. The colony numbers were calculated as mean ± SD. *$p < 0.05$, **$p < 0.01$, ***$p < 0.001$, n = 3, Student's t test. (L) IB analysis of WCLs derived from the HBL cells that were infected with the indicated lentiviral constructs.

(M and N) HBL cell lines generated in (L) were injected into the nude mice (*n = 7* for each group). Tumor volumes were monitored for the indicated time periods (M). The weights of the dissected tumors in Figure S2G were measured and calculated in (N). The data were presented as mean ± SD. **$p < 0.01$, Student's t test. See also Figure S2.
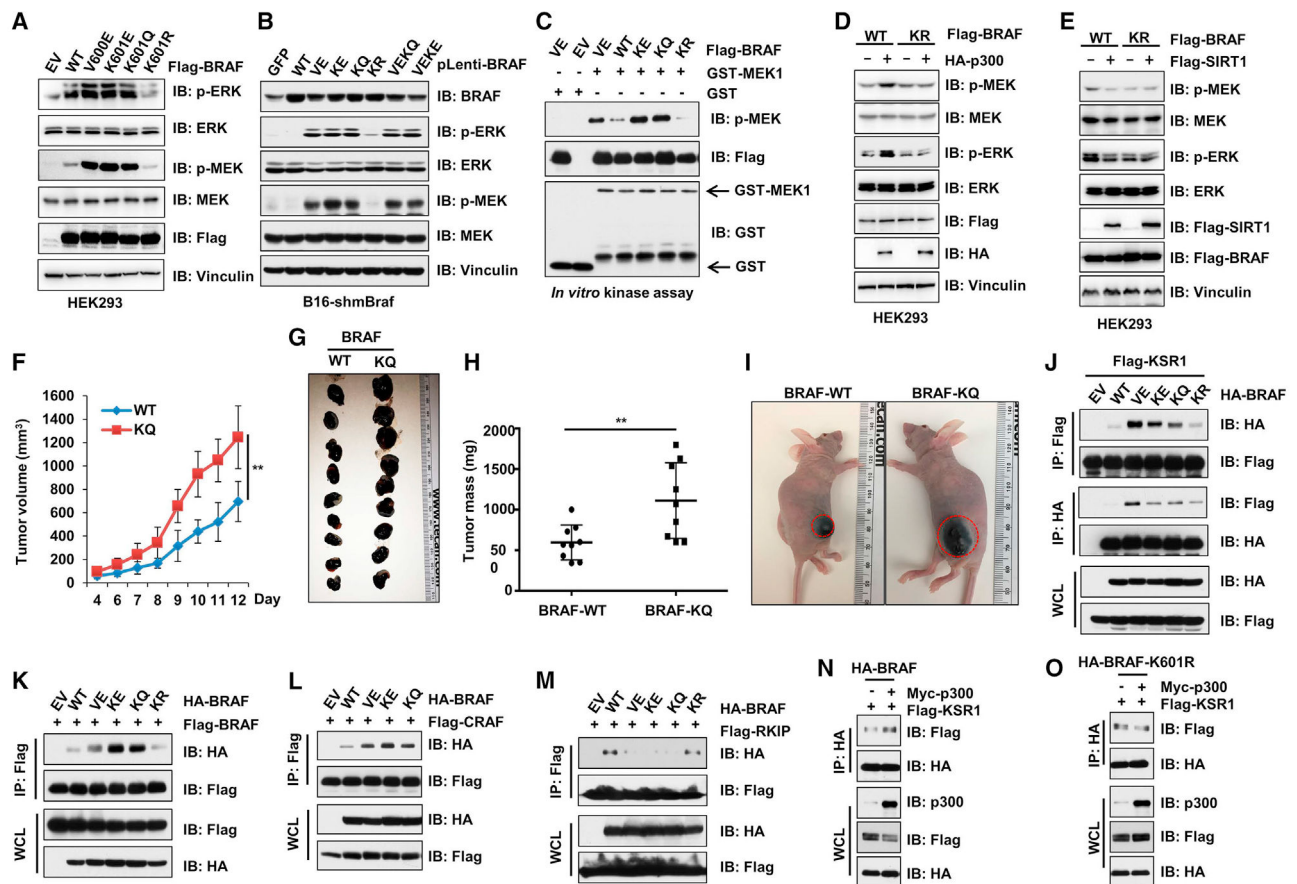
Figure 3. Acetylation of BRAF-K601 enhances BRAF kinase activity

(A) Immunoblot (IB) analysis of WCLs derived from HEK293 cells transfected with the indicated FLAG-BRAF constructs.

(B) IB analysis of WCLs derived from B16 cells infected with the indicated lentiviral constructs. The infected cells were selected with 200 μg/mL hygromycin for 72 h before harvest.

(C) *In vitro* kinase assays showing that compared to WT-BRAF, the kinase activity for V600E-, K601E-, and K601Q-BRAF was markedly elevated in phosphorylating GST-MEK1.

(D and E) IB analysis of WCLs derived from HEK293 cells transfected with HA-p300 (D) or FLAG-SIRT1 (E) and the indicated FLAG-BRAF constructs.

(F) B16 cells stably expressing the WT- or K601Q-BRAF were inoculated subcutaneously into the nude mice ($n = 9$ for each group). *In vivo* tumor growth was monitored over the indicated time period. The tumor volumes were calculated as mean ± SD; **$p < 0.01$, Student's t test.

(G) Subcutaneous tumors formed from the B16 cells (F) stably expressing the WT- and K601Q-BRAF were dissected at the endpoint, and the tumor sizes were compared.

(H) The weights of the dissected tumors in (G). The weights of the tumors were calculated as mean ± SD; **p < 0.01, n = 9, Student's t test.

(I) Representative picture of the tumor-bearing mice as described in (F).

(J–M) IB analysis of WCLs and anti-FLAG IPs derived from HEK293 cells transfected with FLAG-KSR1 (J), FLAG-BRAF (K), FLAG-CRAF (L), or FLAG-RKIP (M) and the indicated HA-BRAF constructs.

(N and O) IB analysis of WCLs and IPs derived from the HEK293 cells transfected with FLAG-KSR1, Myc-p300, and the indicated HA-BRAF constructs.
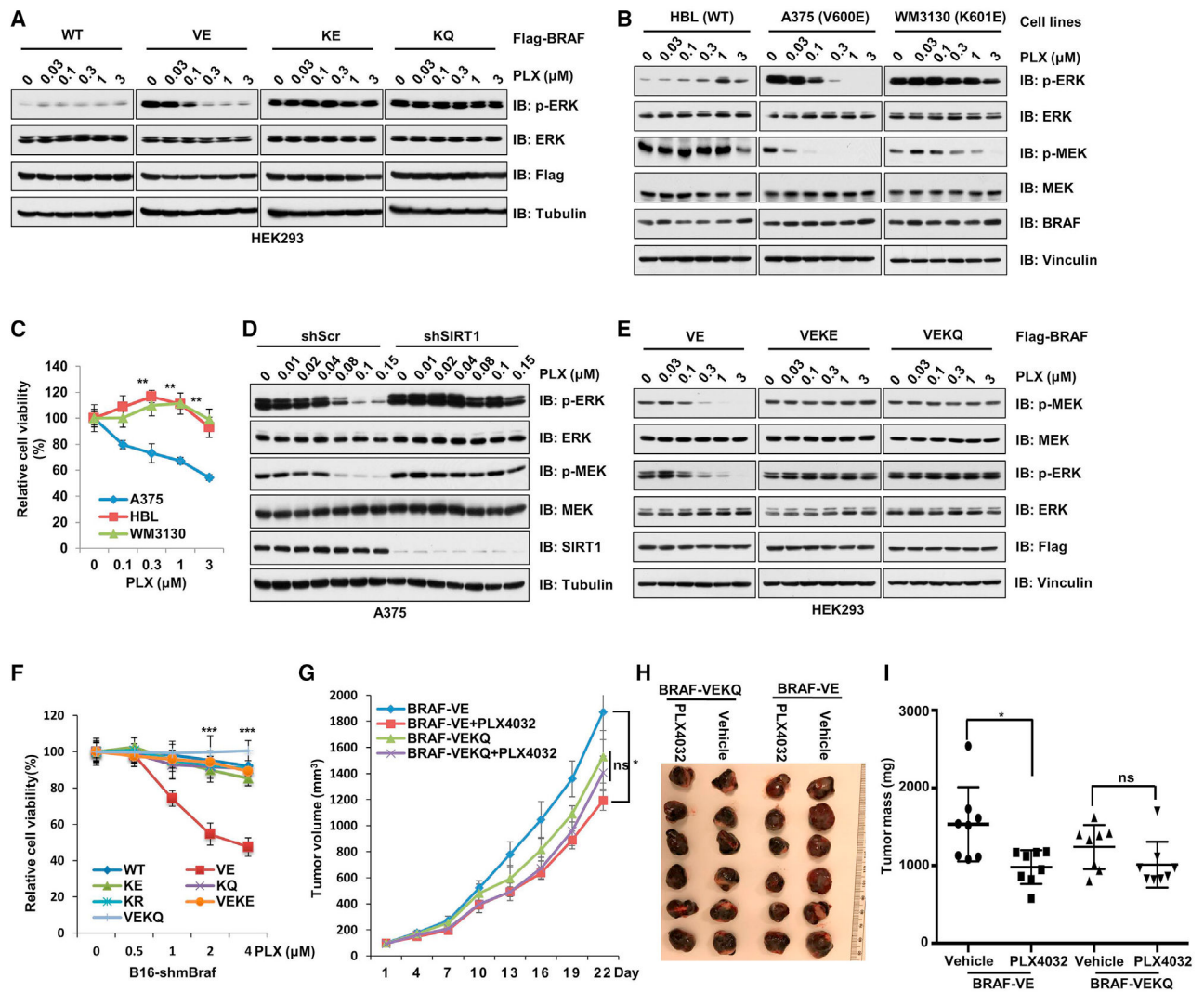
See also Figure S3.

Figure 4. BRAF K601 acetylation contributes to PLX4032 resistance in BRAF^{V600E} harboring melanoma cells

(A) Immunoblot (IB) analysis of whole-cell lysates (WCL) derived from HEK293 cells transfected with the indicated FLAG-BRAF constructs. Cells were treated with indicated concentrations of PLX4032 for 1 h before harvest.

(B) IB analysis of WCLs derived from HBL, A375, and WM3130 cells. Cells were treated with indicated concentrations of PLX4032 for 1 h before harvest.

(C) Cell viability of HBL, A375, and WM3130 cells treated with indicated concentrations of PLX4032 for 48 h. Data are shown as mean ± SD for three technical replicates. **$p < 0.01$, n = 3, Student's t test.

(D) IB analysis of WCLs derived from A375 cells infected with the indicated lentiviral constructs. The infected cells were selected with 1 μg/mL puromycin for 72 h and were treated with the indicated concentration of PLX4032 for 1 h before harvest.

(E) IB analysis of WCLs derived from 293 cells transfected with the indicated constructs. Cells were treated with the indicated concentration of PLX4032 for 1 h before harvest.

(F) Cell viability of B16 cells stably expressing the indicated BRAF-WT and mutants that were treated with the indicated concentration of PLX4032 for 48 h. Data are shown as mean ± SD for three technical replicates. ***$p < 0.001$, n = 3, Student's t test.

(G) B16 cells stably expressing the V600E– or V600E + K601Q-BRAF double mutants were inoculated subcutaneously into the nude mice ($n = 6$ for each group). *In vivo* tumor growth was monitored over the indicated time period. The tumor volumes were calculated as mean ± SD; *$p < 0.05$, n = 8, Student's t test.

(H) Subcutaneous tumors formed from the B16 cells expressing V600E-BRAF and V600E + K601Q-BRAF were dissected at the endpoint, and the tumor sizes were compared.

(I) The weights of the dissected tumors in (H). The weights of the tumors were calculated as mean ± SD; *$p < 0.05$, n = 8, Student's t test.

ns, no significant difference. See also Figure S4.

KEY RESOURCES TABLE

REAGENT or RESOURCE	SOURCE	IDENTIFIER
Antibodies		
Rabbit monoclonal Anti-Akt (Ser473)	Cell Signaling Technology	Cat#4060; RRID: AB_2315049
Rabbit monoclonal Anti-Akt (Thr308)	Cell Signaling Technology	Cat#2965; RRID: AB_2255933
Rabbit monoclonal Anti-pan-Akt1	Cell Signaling Technology	Cat#4691; RRID: AB_915783
Rabbit polyclonal Anti-Acetylated Lysine	Cell Signaling Technology	Cat#9441; RRID: AB_331805
Rabbit polyclonal Anti-ARAF	Cell Signaling Technology	Cat#4432; RRID: AB_330813
Mice monoclonal Anti-BRAF (F7)	Santa Cruz	Cat#sc-5284; RRID: AB_2721130
Rabbit monoclonal Anti-GST	Cell Signaling Technology	Cat#2625; RRID: AB_490796
Rabbit polyclonal Anti-CRAF	Cell Signaling Technology	Cat#9422; RRID: AB_390808
Rabbit polyclonal Anti-MEK1/2	Cell Signaling Technology	Cat#9122; RRID: AB_823567
Rabbit polyclonal Anti-SIRT1	Cell Signaling Technology	Cat#2493; RRID: AB_2188359
Rabbit monoclonal Anti-ERK1/2	Cell Signaling Technology	Cat#9102; RRID: AB_330744
Rabbit monoclonal Anti-pERK1/2	Cell Signaling Technology	Cat#9101; RRID: AB_331646
Rabbit polyclonal Anti-pS217/pS221-MEK1/2	Cell Signaling Technology	Cat#9154; RRID: AB_2138017
Mouse monoclonal Anti-GFP	Clontech	Cat#632375; RRID: AB_2756343
Mouse monoclonal Vinculin	Sigma	Cat#V4505; RRID: AB_477617
Anti-BRAF agarose beads	Santa Cruz	Cat#sc-5284 AC; RRID: N/A
Rabbit polyclonal Anti-HA	Santa Cruz	Cat#sc-805; RRID: AB_631618
Glutathione SEPHAROSE 4B	GE Healthcare	Cat#17-0756-05
Rabbit polyclonal Anti-Flag	Sigma	Cat#F-7425; RRID: AB_439687
Mouse monoclonal Anti-Flag, clone M2	Sigma	Cat#F-3165; RRID: AB_259529
Mouse monoclonal Anti-Tubulin antibody	Sigma	Cat#T-5168; RRID: AB_477579
Anti-Flag agarose beads	Sigma	Cat#A-2220; RRID: AB_10063035
Anti-HA agarose beads	Sigma	Cat#A-2095; RRID: AB_257974
Peroxidase-conjugated anti-mouse secondary antibody	Sigma	Cat#A-4416; RRID: AB_258167
Peroxidase-conjugated anti-rabbit secondary antibody	Sigma	Cat#A-4914; RRID: AB_258207
Anti-Purified anti-HA.11 Epitope Tag Antibody	BioLegend	Cat#MMS101P;RRID: AB_10064068
Protein A/G sepharose beads	GE Healthcare	Cat#17061802
Nickel-beads (Ni-NTA)	Qiagen	Cat#30210
Bacterial and virus strains		
E. coli BL21	TIANGEN	Cat#CB105
XL10-Gold	Agilent Technologies	Cat#200315
DH10Bac	Invitrogen	Cat#10361012
Chemical, peptides, and recombinant proteins		
Insulin	Invitrogen	Cat#41400-045
Trichostatin A (TSA)	Sigma	Cat#T8552
EGF	Sigma	Cat#E9644
Nicotinamide (NAM)	Sigma	Cat#N0636

REAGENT or RESOURCE	SOURCE	IDENTIFIER
C646	Selleckchem	Cat#S7152
Resveratrol	Selleckchem	Cat#S1899
IPTG	Sigma	Cat# I6758
Critical commercial assays		
Cell Fractionation Kit	Cell Signaling Technology	Cat#9038
QuikChange XL Site-Directed Mutagenesis Kit	Agilent Technologies	Cat#200516
DNA Extract Solution	Epicentre	Cat#QE09050
celltiter 96 AQueous One Solution Reagent	Promega	Cat#G3582
Deposited data		
Original western blot images	This paper	Mendeley Data: https://doi.org/10.17632/mrr5n938dv.1
Experimental models: Cell lines		
HEK293	Dr. Pier Paolo Pandolfi, Beth Israel Deaconess Medical Center	N/A
HEK293T	Dr. Pier Paolo Pandolfi, Beth Israel Deaconess Medical Center	N/A
IHPM	Dr. Hans Widlund, Brigham and Women's Hospital	N/A
WM3130	Dr. Keiran Smalley, Moffitt Cancer Center	N/A
A375	Dr. David Fisher, Massachusetts General Hospital	N/A
HBL	Dr. David Fisher, Massachusetts General Hospital	N/A
B16	Dr. Rutao Cui, Boston University School of Medicine	N/A
melan-a	Wellcome Trust Functional Genomics Cell Bank at University of London	N/A
MEFs-WT	Dr. Kun-Ping Lu, Beth Israel Deaconess Medical Center	N/A
MEFs-$SIRT1^{-/-}$	Dr. Kun-Ping Lu, Beth Israel Deaconess Medical Center	N/A
SK-MEL-256	MSKCC	N/A
888-MEL	BioVector NTCC Inc.	N/A
1205Lu	Dr. Keiran Smalley, Moffitt Cancer Center	N/A
1205LuR	Dr. Keiran Smalley, Moffitt Cancer Center	N/A
WM164	Dr. Keiran Smalley, Moffitt Cancer Center	N/A
WM164R	Dr. Keiran Smalley, Moffitt Cancer Center	N/A
YUQUEST	Dr. Ruth Halaban, Yale University School of Medicine	N/A
Experimental models: Organisms/strains		
Nude mice, female	Taconic	NCRNU-M-M
Recombinant DNA		
HA-p300 plasmid	Addgene	Cat#89094
Flag-Tip60α plasmid	Nihira et al., 2017	N/A
HA-CBP plasmid	Inuzuka et al., 2012	N/A
Flag-GCN5 plasmid	Addgene	Cat#74784

REAGENT or RESOURCE	SOURCE	IDENTIFIER
Flag-PCAF plasmid	Addgene	Cat#8941
Flag-BRAF plasmid	Wan et al., 2017	N/A
HA-BRAF plasmid	Wan et al., 2017	N/A
Flag-ARAF plasmid	Wan et al., 2017	N/A
Flag-CRAF plasmid	Wan et al., 2017	N/A
pCMV-GST plasmid	This paper	N/A
Flag-SIRT1 plasmid	Addgene	Cat#13812
Flag-SIRT2 plasmid	Addgene	Cat#13813
Flag-SIRT3 plasmid	Addgene	Cat#13814
Flag-SIRT4 plasmid	Addgene	Cat#13815
Flag-SIRT5 plasmid	Addgene	Cat#13816
Flag-SIRT6 plasmid	Addgene	Cat#13817
Flag-SIRT7 plasmid	Addgene	Cat#13818
Flag-BRAF-K601R plasmid	This paper	N/A
Flag-BRAF-V600E plasmid	Wan et al., 2017	N/A
Flag-BRAF-K601Q plasmid	This paper	N/A
Flag-BRAF-K601E plasmid	This paper	N/A
Flag-BRAF-V600EK601E plasmid	This paper	N/A
Flag-BRAF-V600EK601Q plasmid	This paper	N/A
Flag-BRAF-K253R	This paper	N/A
Flag-BRAF-K418R	This paper	N/A
Flag-BRAF-K418Q	This paper	N/A
Flag-BRAF-K473R	This paper	N/A
Flag-BRAF-K680R	This paper	N/A
Flag-SIRT1-H363Y plasmid	Our lab	N/A
pBabe-SIRT1-WT	Our lab	N/A
pBabe-SIRT1-H363Y	Our lab	N/A
Flag-KSR1 plasmid	Our lab	N/A
Flag-RKIP plasmid	Dr. Kam C. Yeung, the University of Toledo	N/A
HA-NRas plasmid	Dr. Kevin Haigis, Dana-Farber Cancer Institute	N/A
HA-KRas plasmid	Dr. Kevin Haigis, Dana-Farber Cancer Institute	N/A
PGEX-4T-1-NRas	Our lab	N/A
PGEX-4T-1-MEK1	Our lab	N/A
pLKO1-shSIRT1	OpenBiosystems	Cat# RHS4533-EG23411
pLKO1-shBRAF human	OpenBiosystems	Cat#RHS4533-EG4157
pLKO1-shBRAF mouse	OpenBiosystems	Cat#RMM4534-EG17199
pLKO1-shp300	OpenBiosystems	Cat#RHS4533-EG2033
pLenti-BRAF-WT	Wan et al., 2017	N/A
pLenti-BRAF-V600E	Wan et al., 2017	N/A
pLenti-BRAF-K601Q	This paper	N/A
pLenti-BRAF-K601E	This paper	N/A

REAGENT or RESOURCE	SOURCE	IDENTIFIER
pLenti-BRAF-K601R	This paper	N/A
pLenti-BRAF-V600EK601E	This paper	N/A
pLenti-BRAF-V600EK601Q	This paper	N/A
Software and algorithms		
GraphPad Prism	GraphPad	https://www.graphpad.com

Author Manuscript

Author Manuscript

Author Manuscript

Author Manuscript